 DOI: 10.1111/risa.12350

A Risk Assessment Scheme of Infection Transmission Indoors Incorporating the Impact of Resuspension

Siming You[1] and Man Pun Wan[2,*]

A new risk assessment scheme was developed to quantify the impact of resuspension to infection transmission indoors. Airborne and surface pathogenic particle concentration models including the effect of two major resuspension scenarios (airflow-induced particle resuspension [AIPR] and walking-induced particle resuspension [WIPR]) were derived based on two-compartment mass balance models and validated against experimental data found in the literature. The inhalation exposure to pathogenic particles was estimated using the derived airborne concentration model, and subsequently incorporated into a dose-response model to assess the infection risk. Using the proposed risk assessment scheme, the influences of resuspension towards indoor infection transmission were examined by two hypothetical case studies. In the case of AIPR, the infection risk increased from 0 to 0.54 during 0–0.5 hours and from 0.54 to 0.57 during 0.5–4 hours. In the case of WIPR, the infection risk increased from 0 to 0.87 during 0–0.5 hours and from 0.87 to 1 during 0.5–4 hours. Sensitivity analysis was conducted based on the design-of-experiments method and showed that the factors that are related to the inspiratory rate of viable pathogens and pathogen virulence have the most significant effect on the infection probability under the occurrence of AIPR and WIPR. The risk assessment scheme could serve as an effective tool for the risk assessment of infection transmission indoors.

KEY WORDS: Exposure analysis; infection transmission; mass balance model; resuspension; risk assessment

NOMENCLATURE

a_1 Entrance rate of outdoor particles (1/s)
a_2 Entrance rate of resuspended particles (1/s)
$a\prime_2$ $a'_2 = \frac{a_2 N_0 S_v r_{n1}}{Q_s}$
a_r Coefficient in power law function of resuspension rate
b_r Exponent in power law function of resuspension rate
A_{132} Hamaker constant (J)
A_c Area of indoor ceiling (m^2)
A_f Area of indoor floor (m^2)
A_w Area of indoor wall (m^2)
b Loss rate of indoor particles (1/s)
C_i Indoor airborne particle concentration ($\mu g/m^3$) or ($\#/m^3$)
C_o Outdoor airborne particle concentration ($\mu g/m^3$) or ($\#/m^3$)
C_{ov} Airborne particle concentration in the ventilation duct due to AIPR ($\mu g/m^3$) or ($\#/m^3$)
d_{ae} Aerodynamic diameter of pathogens (m)
d_p Particle diameter (m)
d_{v1} Parameter accounting for the effect of particle deposition in the ventilation duct for outdoor particles

[1]Department of Civil & Environmental Engineering, Massachusetts Institute of Technology, Cambridge MA, USA.
[2]School of Mechanical and Aerospace Engineering, Nanyang Technological University, Nanyang, Singapore.
*Address correspondence to School of Mechanical and Aerospace Engineering, Nanyang Technological University, Nanyang 639798, Singapore; tel: +65-6790-5498; fax: +65-6792-4062; mpwan@ntu.edu.sg.

d_{v2} Parameter accounting for the effect of particle deposition in the ventilation duct for the particles from AIPR
d_{v3} Parameter accounting for the effect of particle deposition in the ventilation duct for the particles in the recirculated air
E Indoor constant emission sources besides WIPR
I Amount of pathogens human is exposed to
m_p Mass of a particle (kg)
M Surface particle concentration ($\mu g/m^2$) or ($\#/m^2$)
n_p Number of occupants indoors
N_0 Particle surface number concentration in the ventilation duct ($\#/m^2$)
p_{b1} Aerosol penetration through bends in the ventilation duct for outdoor particles
p_{b2} Aerosol penetration through bends in the ventilation duct for resuspended particles
p_{b3} Aerosol penetration through bends in the ventilation duct for the particles in the recirculated air
p_c Penetration coefficient of particles through building shell
P_c Width of the ceiling of ventilation duct (m)
P_f Width of the floor of ventilation duct (m)
p_{fi} Inhalability parameter accounting for the real exposure to pathogens
p_{fs} Fraction of pathogens survived
P_i Infection probability
P_w Width of the wall of ventilation duct (m)
Q_s Ventilation rate (m^3/s)
r_i Fitting parameter accounting for the infectivity of pathogen and the pathogen-host interactions in the exponential dose-response model
r_{n1} Coefficient in the power law function of normalized resuspension rate
r_{n2} Exponent in the power law function of normalized resuspension rate
R Resuspension rate ($\mu g/s$) or ($\#/s$)
R_r Fraction of recirculated air from the exiting air
S_r Particle resuspension area (m^2)
S_v Dose area of BW in the ventilation duct (m^2)
t Time (s)
T_e Exposure period (s)
u^* Friction velocity (m/s)
v_{df} Particle deposition velocity onto floor (m/s)
v_{dw} Particle deposition velocity onto wall (m/s)
v_{dc} Particle deposition velocity onto ceiling (m/s)
v_{dfv} Particle deposition velocity onto the floor of ventilation duct (m/s)
v_{dwv} Particle deposition velocity onto the wall of ventilation duct (m/s)
v_{dcv} Particle deposition velocity onto the ceiling of ventilation duct (m/s)
V Volume of indoor space (m^3)
x_{v1} Ventilation duct length passed by the entering outdoor particles (m)
x_{v2} Ventilation duct length passed by the resuspended particles (m)
x_{v3} Ventilation duct length passed by the particles in the recirculated air (m)

Greek symbols

α_a Air exchange rate (1/s)
β_b Breathing rate of an occupant (m^3/s)
γ_d Decay rate of pathogen (1/s)
η_r Removal efficiency of filter in the ventilation duct
Λ Normalized resuspension rate (1/s)
σ_1 Roughness of surface (m)
ρ_a Density of air (kg/m^3)
ρ_p Density of particle (kg/m^3)

1. INTRODUCTION

Outbreaks of infectious disease have caused massive civilian casualties. Despite the significant improvement of modern medicine and living standards, some of these diseases continually impose great threat to the lives of human beings. For instance, there were an estimated 8.3 million new tuberculosis (TB) cases in 2000[1] and more than 40,000 TB-related deaths annually in industrialized nations.[2] Some emerging infectious diseases bring further threat to humans since the relevant control and management knowledge is generally lacking by the time they break out. A typical example is the outbreak of severe acute respiratory syndrome (SARS) during 2002–2003, which caused great panic in the public because of the high fatality rate of the disease.[3]

The anthrax letter incidents of 2001 in the United States raised an additional concern about the spread of infection by bioterrorist attacks. Bioterrorist attacks by the intentional release of aerosolized biological agents are characterized by their relatively low costs and technical challenges, the capability of causing injury and death in strange and prolonged ways, and their potential to inflict huge economic loss.[4] It was estimated that the postattack cost could be as

high as $26.2 billion per 100,000 persons exposed to biological agents.[5]

People spend most of their time (70%–90%) indoors; therefore, it is important to develop the capability to analyze human exposure to pathogens and thus infection risk for indoor environments.[6] Generally, there are three major infection transmission modes indoors, that is, droplet, airborne, and contact mode.[7,8] Indoor surfaces serve as sinks for airborne pathogens because of deposition. However, some of these deposited pathogens could maintain their infectivity for extended periods (e.g., from several hours to months).[9–11] Once these deposited pathogens are resuspended from surfaces and become airborne again, they may be inhaled by occupants and impose a secondary infection risk. Previous studies[12–15] suggested that pathogen resuspension can be a potential route for infection transmission. For example, Goebes *et al.*[15] found that walking over carpet could significantly increase the airborne concentration of *Aspergillus* and potentially result in invasive aspergillosis that could be fatal for immunocompromised people. Nazaroff[13] also indicated that the fomite on a heavily trafficked floor might become a secondary source of airborne pathogens because of human walking.

Risk assessment is commonly adopted to preclude infection and handle postepidemic or postattack situations.[16] A large number of studies have been done[17–24] to develop risk assessment models for infection transmission. However, very few of these studies[19,24] explored the infection transmission route via pathogen resuspension. Resuspension rates (the amount of particles resuspended per unit time) were generally assumed to be constant in these analyses for simplicity, despite the fact that resuspension rates should vary with respect to time.[25–27] Hence, the capability of quantitatively characterizing the influence of pathogen resuspension toward infection transmission is still limited. This study aims to shed new insight into infection control and management based on risk assessment by proposing a new risk assessment scheme that quantifies the impact of resuspension to infection transmission indoors.

2. MODEL DEVELOPMENT

2.1. Identification of Resuspension Scenarios

Particle resuspension is governed by the interaction between detachment forces and adhesion forces. Depending on the source of detachment forces, there are airflow-induced particle resuspension (AIPR) and human-activity-induced particle resuspension (HAIPR), both of which are associated with human exposure to particles in the indoor environment.

Previous studies observed that the initiation friction velocity below which AIPR could not occur ranged from 0.1 to 0.3 m/s for particles of 1–34 μm[28–30] and the initiation friction velocity is generally larger for smaller particles.[31] The characteristic friction velocity in indoor environments ranges from 0.01 to 0.03 m/s[32] and the particles that are associated with human inhalation exposure are generally smaller than 10 μm, suggesting that AIPR in an indoor environment could hardly be a major contributing mechanism to particle inhalation exposure. In contrast, the characteristic friction velocity in ventilation air ducts is much higher (e.g., 0.7 m/s for a typical average airflow velocity of 9 m/s in the duct[33]), indicating that AIPR in the ventilation air ducts is highly probable. Specifically, the particle resuspension in ventilation air ducts is relevant to ventilation-system-targeted bioterrorist attacks where harmful agents could be deliberately dosed onto the duct floor when the ventilation system is off (usually at night, therefore more covert). Once the ventilation system is turned on again, some of these dosed agents could be resuspended and transported into the indoor environment, leading to mass contamination.[34–37] The U.S. government warned that the ventilation systems of buildings are an ideal target for bioterrorism.[37]

The AIPR in ventilation ducts could be considered by introducing the particle concentration dynamics model developed by You and Wan[38] into the two-compartment mass balance models of indoor particle dynamics. According to the study of You and Wan,[38] the particle concentration in the duct with the occurrence of AIPR without considering particle deposition in the duct is:

$$C_{ov}(t) = \frac{N_0 S_v \Lambda}{Q_s}, \tag{1}$$

where N_0 is the surface number concentration of pathogens dosed onto the floor of duct, S_v is the area of floor dosed with pathogens, and 2.83×10^{-4} is the ventilation rate in the duct. $\Lambda = r_{n1} t^{-r_{n2}}$ is the normalized resuspension rate (the fraction of particles resuspended per unit time) for AIPR. The normalized resuspension rate (Λ) could be calculated by the model from Loosmore:[26]

$$\Lambda = 0.42 \frac{u^{*2.13} d_p^{0.17}}{t^{0.92} \sigma_1^{0.32} \rho_p^{0.76}} \quad (2)$$

or that from Kim *et al.*:[25]

$$\frac{\Lambda d_p}{u^*} = 8.521 \times 10^{-3} \left(\frac{\rho_p}{\rho_a}\right)^{-0.3028} \times \left(\frac{u^* t}{d_p}\right)^{-1.0135} \left(\frac{\sigma_1}{d_p}\right)^{-0.3269} \left(\frac{A_{132}}{d_p^{3u^{*2}} \rho_a}\right)^{-0.2961}, \quad (3)$$

where u^* is the friction velocity, ρ_p is the particle density, ρ_a is the air density, $A_{132} = \sqrt{A_{11} A_{22}}$ (A_{11} and A_{22} are the Hamaker constant of particle and surface, respectively) is the Hamaker constant, d_p is the particle diameter, σ_1 is the surface roughness, and t is the time. When they are validated against different experiments, Equation (2) shows better match with experimental data than Equation (3) in some datasets, whereas Equation (3) outperforms Equation (2) in some others. There is still no definite conclusion about which model, Equation (2) or (3), is more accurate. After plugging in the case-specific parameters (Table II for this study), both Equations (2) and (3) will arrive at a power law form of $\Lambda = k_1 t^{k_2}$, where k_1 is the coefficient and k_2 is the exponent. The final form for Λ in this study is obtained by taking the average of coefficients and exponents from Equations (2) and (3). The final form of Λ used in this study is shown in Table III.

A variety of human activities could resuspend particles indoors, such as walking, vacuuming, and bed folding. Among these activities, walking (i.e., walking-induced particle resuspension [WIPR]) is one of the most common ones capable of causing significant particle resuspension.[39–43] The field measurement of Weis *et al.*[44] following the 2001 anthrax attack in the United States suggested that the WIPR could serve as one of secondary pathogen sources for human exposure. WIPR is considered by this work as another resuspension scenario. It has been shown that the variation of resuspension rate with respect to time for WIPR could be reasonably described by a power law function:[45]

$$R(t) = a_r t^{-b_r}, \quad (4)$$

where a_r depends on the factors such as walking strength, particle surface loading, relative humidity (RH), resuspension area, and flooring material.[45–47]

The AIPR- and WIPR-related airborne particle concentration models have been developed by You and Wan[38,45] based on a one-compartment mass balance model. In Section 2.2, two-compartment mass balance models will be employed to develop both airborne and surface particle concentration models with the occurrence of both AIPR and WIPR, which serve as the basis for the exposure analysis of Section 2.3 and risk assessment of Section 2.4.

2.2. Airborne and Surface Particle Concentration Models

2.2.1. Two-Compartment Mass Balance Model

Indoor particle concentration profiles could be modeled by two-compartment mass balance models under the well-mixed assumption. The well-mixed assumption has been widely adopted for modeling indoor particle concentration variation.[46,48–50] The two-compartment mass balance models are:

$$\frac{dC_i}{dt} = a_1 C_o + a_2 C_{ov} - b C_i + \frac{R}{V} + \frac{E}{V} \quad (5)$$

$$\frac{dM}{dt} = C_i v_{df} - \frac{R}{S_r} \quad (6)$$

under the initial condition of $C_i(0)$ (#/m^3) and $M(0)$ (#/m^2). Equations (5) and (6) account for the air and surface compartments, respectively. C_i (#/m^3) and C_o (#/m^3) are the indoor and outdoor airborne particle concentrations, respectively. C_{ov} (#/m^3) is the airborne particle concentration in the ventilation duct due to the AIPR inside (Equation (1)). M (#/m^2) is the indoor particle concentration on the surface where resuspension occurs. V (m^3) is the volume of indoor space. R (#/s) is the resuspension rate of WIPR. v_{df} (m/s) is the particle deposition velocity onto the floor. S_r (m^2) is the particle resuspension area. E (#/s) is the indoor emission sources (e.g., expiratory activities) besides WIPR. a_1 (s^{-1}) is the entrance rate of outdoor particles. a_2 (s^{-1}) is the entrance rate of resuspended particles from the ventilation duct. b (s^{-1}) is the loss rate of indoor particles. a_1, a_2, and b are ventilation system dependent (i.e., mechanical ventilation and natural ventilation).

In the case of mechanical ventilation (Fig. 1(a)), $a_1 = (1 - R_r)(1 - \eta_r) p_{b1} d_{v1} \alpha_a$. α_a (s^{-1}) is the air exchange rate. R_r is the fraction of recirculated air from the exiting air. η_r is the removal efficiency of the filter in the ventilation duct, which depends on the particle size and the type of filter. η_r can be obtained from the study of Riley *et al.*[51] for

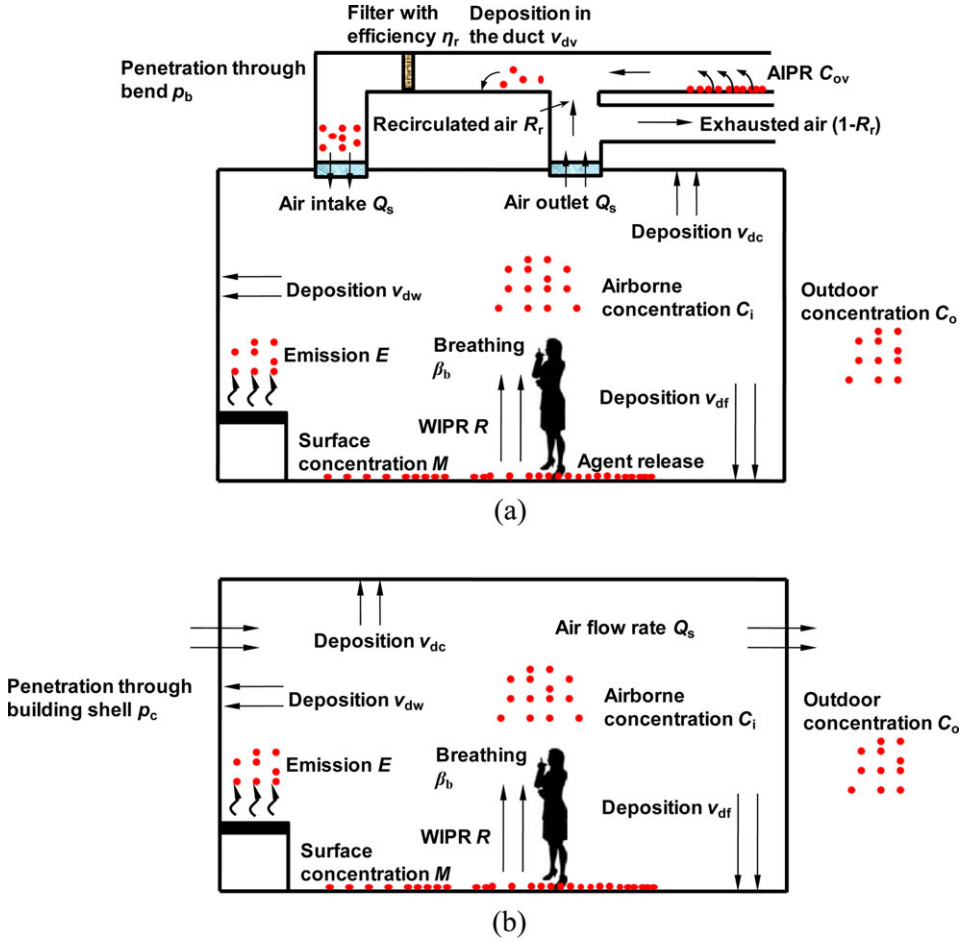

Fig. 1. Schematic diagrams of indoor particle dynamics for (a) mechanical ventilation and (b) natural ventilation.

some commonly used commercial filters such as 40% and 85% ASHRAE filters. p_{b1} is the aerosol penetration through bends in the ventilation duct for outdoor particles and could be estimated according to the theory of McFarland *et al.*[52] d_{v1} is the parameter accounting for the effect of particle deposition in the ventilation duct and is calculated by $d_{v1} = e^{-\frac{(v_{dfv}P_f + v_{dwv}P_w + v_{dcv}P_c)x_{v1}}{(1-R_r)Q_s}}$. v_{dfv}, v_{dwv}, and v_{dcv} are the deposition velocities of particles onto the floor, wall, and ceiling of the ventilation duct, respectively, which could be estimated based on the study by Sippola and Nazaroff.[33] P_f, P_w, and P_c are the width of floor, wall, and ceiling of ventilation duct, respectively. x_{v1} is the ventilation duct length passed by outdoor particles. $Q_s = \alpha_a V$ (m^3/s) is the ventilation rate. $a_2 = (1 - R_r)(1 - \eta_r)p_{b2}d_{v2}\alpha_a$. p_{b2} is the aerosol penetration through bends for resuspended particles in the ventilation duct. $d_{v2} = e^{-\frac{(v_{dfv}P_f + v_{dwv}P_w + v_{dcv}P_c)x_{v2}}{(1-R_r)Q_s}}$. x_{v2} is the ventilation duct length passed by the resuspended particles in the ventilation duct. $b = \alpha_a - R_r d_{v3}(1 - \eta_r)p_{b3}\alpha_a + \frac{(v_{df}A_f + v_{dw}A_w + v_{dc}A_c)}{V} + \frac{\beta_b n_p}{V}$. v_{df} (m/s), v_{dw}(m/s), and v_{dc} (m/s) are the particle deposition velocities onto the indoor floor, wall, and ceiling, respectively, and can be estimated based on the existing model[32] or experimental data.[53] A_f (m^2), A_w(m^2), and A_c (m^2) are the areas of indoor floor, wall, and ceiling, respectively. β_b (m^3/s) is the breathing rate of the occupant. The deposition efficiency of pathogen in human respiratory tract varies from 0.2 to 1 according to the size of the pathogen. In this study, the aerodynamic diameter of *Bacillus anthracis* (considered pathogen) is assumed to be 3 μm. The corresponding deposition efficiency is above 0.9.[54] For simplicity of subsequent analysis, it is assumed to be 1. For other pathogens that have a much lower deposition efficiency, the term $\frac{\beta_b n_p}{V}$ should be multiplied by the deposition efficiency

in the equation of the loss rate (b) to account for the corresponding effect. n_p is the number of occupants. $d_{v3} = e^{-\frac{(v_{dfv}P_f + v_{dwv}P_w + v_{dcv}P_c)x_{v3}}{R_r Q_s}}$ accounts for the deposition of particles in the recirculated air. x_{v3} is the duct length passed by the recirculated air. p_{b3} is the aerosol penetration through bends in the ventilation duct for the particles in the recirculated air.

In the case of natural ventilation (Fig. 1(b)), $a_1 = p_c\alpha_a$. p_c is the penetration coefficient ranging from 0 to 1 depending on the factors such as particle size and building conditions. The penetration coefficient could be estimated based on existing size-resolved experimental data.[48,55–57] $a_2 = 0$, that is, AIPR from the ventilation duct, does not exist in the case of natural ventilation. $b = \alpha_a + \frac{(v_{df}A_f + v_{dw}A_w + v_{dc}A_c)}{V} + \frac{\beta_b n_p}{V}$. In Equations (5) and (6), particle coagulation and condensation are not considered. Wherever the effect of coagulation or condensation becomes significant (e.g., extremely high airborne particle concentration such as more than 1×10^{10} #/m^3[58]), the model needs to be modified to account for the corresponding effect. In Equations (5) and (6), the parameters are corresponding to the particles within a certain size bin, which allows the particle size distribution to be considered implicitly. For example, if there are different particle size classes, each class of particles will have its own set of mass balance models and the combination of all sets of mass balance models will describe the particle dynamics of all these particles.

To solve Equations (5) and (6), the information about the dynamics of outdoor concentration (C_o) and other emission sources (E) is needed. The outdoor concentration is assumed to be zero because most of pathogens could not survive for a long period of time outdoors because of the germicidal effect of sunlight.[59] For other indoor emission sources such as expiratory activities and aerosolization of harmful pathogens during a bioterrorist attack, the emission dynamics is controlled by the particle producing process. The emission rate, E (the number or mass of particles emitted per unit time) of these sources is assumed to be constant (i.e., $E = D$) during the period of emission, which has also been adopted by existing studies.[23,60–62]

2.2.2. *Airborne and Surface Particle Concentration Models*

Substituting $C_o(t) = 0$, $C_{ov}(t) = \frac{N_0 S_v r_{n1}}{Q_s t^{r_{n2}}}$, $R(t) = a_r t^{-b_r}$, and $E = D$ into Equation (5) yields:

$$\frac{dC_i}{dt} = a_2\left(\frac{N_0 S_v r_{n1}}{Q_s t^{r_{n2}}}\right) - bC_i + \frac{a_r}{Vt^{b_r}} + \frac{D}{V}. \quad (7)$$

Substituting $R(t) = a_r t^{-b_r}$ into Equation (6) yields:

$$\frac{dM}{dt} = C_i v_{df} - \frac{a_r}{S_r t^{b_r}}. \quad (8)$$

Let $\frac{a_2 N_0 S_v r_{n1}}{Q_s} = a_2'$; Equation (7) becomes:

$$\frac{dC_i}{dt} = a_2' t^{-r_{n2}} - bC_i + \frac{a_r}{Vt^{b_r}} + \frac{D}{V}. \quad (9)$$

The indoor airborne particle concentration is obtained by solving Equation (9) as:

$$C_i(t) = e^{-bt}C_i(0) + a_2' e^{-bt}\int_0^t \frac{e^{bt}}{t^{r_{n2}}}dt + \frac{a_r}{V}e^{-bt}\int_0^t \frac{e^{bt}}{t^{b_r}}dt + \frac{D}{V}(1 - e^{-bt}). \quad (10)$$

Putting Equation (10) back into Equation (8) and integrating with respect to time from 0 to t gives the surface particle concentration:

$$M(t) = M(0) + \frac{v_{df}C_i(0)}{b}(1 - e^{-bt}) - \frac{a_r}{S_r(1 - b_r)}t^{1-b_r} + v_{df}a_2'\int_0^t \left\{e^{-bt}\left[\int_0^t \frac{e^{b\tau}}{(\tau)^{r_{n2}}}d\tau\right]\right\}dt + \frac{v_{df}a_r}{V}\int_0^t \left\{e^{-bt}\left[\int_0^t \frac{e^{b\tau}}{\tau^{b_r}}d\tau\right]\right\}dt + \frac{v_{df}D}{V}t - \frac{v_{df}D}{Vb}(1 - e^{-bt}). \quad (11)$$

Applying the theorem of integration by parts to the fourth and fifth terms on the right-hand side of Equation (11) yields:

$$M(t) = M(0) + \frac{v_{df}C_i(0)}{b}(1 - e^{-bt}) - \frac{a_r}{S_r(1 - b_r)}t^{1-b_r} + \frac{v_{df}a_2'}{b}\left[\int_0^t \frac{1}{t^{r_{n2}}}dt - e^{-bt}\int_0^t \frac{e^{bt}}{t^{r_{n2}}}dt\right] + \frac{v_{df}a_r}{Vb}\left[\int_0^t \frac{1}{t^{b_r}}dt - e^{-bt}\int_0^t \frac{e^{bt}}{t^{b_r}}dt\right]$$

$$+\frac{v_{\mathrm{df}}D}{V}t-\frac{v_{\mathrm{df}}D}{Vb}(1-e^{-bt})$$
$$=M(0)+\frac{v_{\mathrm{df}}C_{\mathrm{i}}(0)}{b}-\frac{a_{\mathrm{r}}}{S_{\mathrm{r}}(1-b_{\mathrm{r}})}t^{1-b_{\mathrm{r}}}$$
$$+\frac{v_{\mathrm{df}}a_2'}{b(1-r_{\mathrm{n2}})}t^{1-r_{\mathrm{n2}}}+\frac{v_{\mathrm{df}}a_{\mathrm{r}}}{Vb(1-b_{\mathrm{r}})}t^{1-b_{\mathrm{r}}}$$
$$-\frac{v_{\mathrm{df}}C_{\mathrm{i}}(t)}{b}+\frac{v_{\mathrm{df}}D}{V}t. \quad (12)$$

The effect of each source on the variation of airborne and surface concentrations could be identified based on the derived models (Equations (10) and (12)). For example, the airborne concentration model (Equation (10)) consists of four terms. The first term accounts for the effect of initial indoor airborne concentration. The second and third terms account for the effect of AIPR in the ventilation duct and WIPR indoors, respectively. The fourth term accounts for the effect of other indoor emission sources. The indoor particle loss mechanisms (e.g., deposition and ventilation) denoted by b affect all four terms in an exponential way. The airborne concentration is resultant from the superposition of initial concentration, AIPR, WIPR, and other indoor emission sources under the effect of these loss mechanisms. The contribution of AIPR and WIPR toward indoor airborne and surface concentrations under a certain ventilation, building, and occupancy conditions could be identified based on the above models.

2.3. Exposure Analysis

Because inhalation infection risk is generally the main component of overall infection risk[19] and is the major risk associated with resuspension, only inhalation exposure is considered here. The inhalation exposure during a period of T_{e} can be calculated as:

$$I=\beta_{\mathrm{b}}p_{\mathrm{fi}}p_{\mathrm{fs}}\int_0^{T_{\mathrm{e}}}C_{\mathrm{i}}(t)dt, \quad (13)$$

where p_{fs} is the fraction of pathogens survived after a certain period of time, which can be estimated by $p_{\mathrm{fs}}=e^{-\gamma_{\mathrm{d}}t}$ with γ_{d} as the decay rate of pathogen.[63] $p_{\mathrm{fi}}=1-0.15[\log_{10}(1+d_{\mathrm{ae}})]^2-0.10\log_{10}(1+d_{\mathrm{ae}})$ is the inhalability parameter, where d_{ae} is the aerodynamic diameter of pathogens.[64] For the pathogen concerned in this study (*B. anthracis*), which has an aerodynamic diameter of 3 μm, the inhalability parameter is very close to 1.

To estimate the inhalation exposure, the airborne concentration model (Equation (10)) is substituted into the integral of Equation (13), $\int_0^{T_{\mathrm{e}}}C_{\mathrm{i}}(t)dt$, leading to,

$$\int_0^{T_{\mathrm{e}}}C(t)\,dt=\frac{C_{\mathrm{i}}(0)}{b}+\frac{a_2'}{b(1-r_{\mathrm{n2}})}T_{\mathrm{e}}^{1-r_{\mathrm{n2}}}$$
$$+\frac{a_{\mathrm{r}}}{Vb(1-b_{\mathrm{r}})}T_{\mathrm{e}}^{1-b_{\mathrm{r}}}-\frac{C_{\mathrm{i}}(T_{\mathrm{e}})}{b}+\frac{D}{V}T_{\mathrm{e}}$$
$$=\frac{M(T_{\mathrm{e}})-M(0)+\frac{a_{\mathrm{r}}}{S_{\mathrm{r}}(1-b_{\mathrm{r}})}T_{\mathrm{e}}^{1-b_{\mathrm{r}}}}{v_{\mathrm{df}}}, \quad (14)$$

and thus the exposure estimation is:

$$I=\beta_{\mathrm{b}}p_{\mathrm{fi}}p_{\mathrm{fs}}\left\{\frac{C_{\mathrm{i}}(0)}{b}+\frac{a_2'}{b(1-r_{\mathrm{n2}})}T_{\mathrm{e}}^{1-r_{\mathrm{n2}}}\right.$$
$$\left.+\frac{a_{\mathrm{r}}}{Vb(1-b_{\mathrm{r}})}T_{\mathrm{e}}^{1-b_{\mathrm{r}}}-\frac{C_{\mathrm{i}}(T_{\mathrm{e}})}{b}+\frac{D}{V}T_{\mathrm{e}}\right\}$$
$$=\beta_{\mathrm{b}}p_{\mathrm{fi}}p_{\mathrm{fs}}\left[\frac{M(T_{\mathrm{e}})-M(0)+\frac{a_{\mathrm{r}}}{S_{\mathrm{r}}(1-b_{\mathrm{r}})}T_{\mathrm{e}}^{1-b_{\mathrm{r}}}}{v_{\mathrm{df}}}\right]. \quad (15)$$

It should be noted that in the case without WIPR, $\int_0^{T_{\mathrm{e}}}C(t)\,dt=\frac{M(T_{\mathrm{e}})-M(0)}{v_{\mathrm{df}}}$, and thus:

$$I=\beta_{\mathrm{b}}p_{\mathrm{fi}}p_{\mathrm{fs}}\left[\frac{M(T_{\mathrm{e}})-M(0)}{v_{\mathrm{df}}}\right]. \quad (16)$$

This means that the inhalation exposure is directly proportional to the pathogen surface concentration in the case without WIPR. Hence, the exposure estimation can be performed based on surface concentration sampling in the case without WIPR, which is of practical significance for postepidemic or postattack responses.

2.4. Infection Probability Analysis

The infection probability after exposure to a certain amount of pathogens could be estimated by the exponential dose-response model:[19,61,65]

$$P_{\mathrm{i}}=1-e^{-r_{\mathrm{i}}I}, \quad (17)$$

where r_{i} is the fitting parameter accounting for the infectivity of pathogen and the pathogen-host interactions. I is the human exposure to pathogens. The influences of various factors (e.g., pathogen persistence, deposition loss of pathogen, and pathogen resuspension) on infection transmission modify the magnitude of human exposure, which changes the input in the dose-response model to give different infection probabilities. Hence, the role of

resuspension in infection transmission could be determined by incorporating the exposure estimation (Equation (15)) into the dose-response model and will be examined by the case studies in Section 4.

3. PHYSICAL VALIDATION

The infection-probability-based model validation is impossible for the time being because of the lacking of relevant data. Alternatively, physical validation is conducted by comparing model predictions of airborne particle concentrations to experimental data[66] (WIPR involved) found in the literature. The validation of AIPR in the ventilation duct is not conducted due to the lacking of experimental data and is left for a future task.

The study of Qian and Ferro[66] measured the variation of airborne particle (0.4–10 μm) concentrations in a full-scaled chamber where a participant performed prescribed activities on a seeded carpet. The participant first walked on the carpet for five minutes, followed by sitting for 20 minutes, and then walked for five minutes again followed by leaving the chamber. The airborne concentration profiles for 2–3 μm and 4–5 μm particles were selected for validation. A HEPA filter was installed upon the chamber ventilation and the outdoor airborne particles did not enter the chamber during the measurements. The test dust was seeded onto the carpet to a mass concentration of 20 g/m^2 based on which the number concentrations of 2–3 μm and 4–5 μm particles can be estimated based on the size distribution of test dust and the particle density (2650 kg/m^3).[45] The surface mass concentrations for 2–3 μm and 4–5 μm particles are ($20 \times 0.13 = 2.6$ g/m^2) and ($20 \times 0.2 = 4$ g/m^2), respectively. The average diameters, 2.5 μm and 4.5 μm, are used to represent 2–3 μm and 4–5 μm particles, respectively, and the corresponding masses (m_p) for 2.5 μm and 4.5 μm spherical particles are 2.17×10^{-5} μg and 1.26×10^{-4} μg, respectively. Hence, the surface number concentrations for 2–3 μm and 4–5 μm particles are 1.20×10^{11} #/m^2 and 3.17×10^{10} #/m^2, respectively. The RH in the experiments was 31.7%. The particle resuspension area is 5.95 m^2. To determine the resuspension rate for the WIPR, the resuspension rate [$R(t) = 2.25t^{-0.58}$] of the carpet/PM_{10} case at the walking rate of 132 steps/min under the RH of 82% in the study of You and Wan[45] is used as the reference. In the reference case, the resuspension area is 0.2 m^2 and the surface mass concentration is 1.75 g/m^2. The power law coefficient (a_r) of resuspension rate is proportional to the resuspension area and particle surface concentration. Based on the study of You and Wan,[45] the normalized resuspension rate under the RH of 31.7% is assumed to be 5–6 times of that under the RH of 82%. The normalized resuspension rate of PM_{10} was about 2.5 times of $PM_{2.5}$ and resuspension is more significant for larger particles.[45] It is assumed that the normalized resuspension rates for the cases of 2–3 μm and 4–5 μm particles are (0.4–0.6) and (0.8–1.0) times that of PM_{10}, respectively. Hence, the power law coefficient of resuspension rate for 2–3 μm particles is estimated to range from ($2.25 \times 5 \times 0.4 \times 2.6 \times 5.95/[0.2 \times 1.75] = 198.9$) to ($2.25 \times 6 \times 0.6 \times 2.6 \times 5.95/[0.2 \times 1.75] = 358.0$) and the corresponding resuspension rate for 2–3 μm particles varies from $R(t) = 198.9t^{-0.58}$ to $R(t) = 358.0t^{-0.58}$ in the unit of μg/s. The power law coefficient of resuspension rate for 4–5 μm particles is approximated to range from ($2.25 \times 5 \times 0.8 \times 5 \times 5.95/[0.2 \times 1.75] = 612.0$) to ($2.25 \times 6 \times 1.0 \times 4 \times 5.95/[0.2 \times 1.75] = 918.0$) and the corresponding resuspension rate for 4–5 μm particles varies from $R(t) = 612.0t^{-0.58}$ to $R(t) = 918.0t^{-0.58}$ in the unit of μg/s. In view that measured airborne concentration was in the unit of #/m^3, the resuspension rate is further divided by the mass of a single particle (m_p) to convert the unit of μg/s to #/s. Hence, the resuspension rates in the unit of #/s vary from $R(t) = 9.2 \times 10^6 t^{-0.58}$ (lower resuspension rate) to $R(t) = 1.7 \times 10^7 t^{-0.58}$ (upper resuspension rate) and from $R(t) = 4.8 \times 10^6 t^{-0.58}$ (lower resuspension rate) to $R(t) = 7.3 \times 10^6 t^{-0.58}$ (upper resuspension rate) for 2–3 μm and 4–5 μm particles, respectively. The parameters required for modeling are listed in Table I. The comparison between experimental data and model predictions is given by Fig. 2. The model predictions are based on the lower and upper resuspension rates, respectively, to account for the uncertainty of resuspension rate estimation.

It is shown that the model predictions based on lower and upper resuspension rate well cover the experimental data and capture the variation of airborne concentrations with respect to time; that is, the concentration quickly increases during the walking period because of the overwhelming effect of WIPR and declines during the nonwalking period because of the particle loss mechanisms (e.g., deposition and ventilation). The increase of airborne concentration for 2.5 μm particles is larger than that for 4.5 μm particles because of the fact that the initial surface concentration is larger for 2.5 μm particles. This is also reflected in Table I where 2.5 μm particles have

Table I. Parameters Used for Model Predictions During the Model Validation

Parameters	Meaning	Reference Study[66]
α_a (1/s)	Air exchange rate	1.11×10^{-4}
p_c	Penetration through building shell	–
R_r	Fraction of recirculated air	0
η_r	Filter efficiency	1
p_b	Penetration through bend(s)	–
d_v	Deposition loss in the duct	–
v_{df} (m/s)	Deposition velocity onto floor	1.0×10^{-3} (2.5 μm) 2.5×10^{-3} (4.5 μm)
v_{dw} (m/s)	Deposition velocity onto wall	9.0×10^{-5} (2.5 μm) 3.0×10^{-5} (4.5 μm)
v_{dc} (m/s)	Deposition velocity onto ceiling	5.0×10^{-6} (2.5 μm) 1.0×10^{-6} (4.5 μm)
A_f (m^2)	Area of indoor upward facing surfaces	17.86
A_w (m^2)	Area of indoor vertical facing surfaces	52.09
A_c (m^2)	Area of indoor downward facing surfaces	17.86
V (m^3)	Volume of indoor space	54.48
β_b(m^3/s)	Breathing rate of occupants	2.83×10^{-4}[a]
n_p	Number of occupants	1
$C_i(0)$ (#/m^3)	Initial indoor airborne concentration	0
$M(0)$ (#/m^2)	Initial indoor surface concentration for resuspension	1.20×10^{11} (2.5 μm) 3.17×10^{10} (4.5 μm)
C_o (#/m^3)	Outdoor concentration	–
R (#/s)	Resuspension rate	$(5.5 \times 10^6 - 1.9 \times 10^7)t^{-0.58}$ (2.5 μm) $(3.4 \times 10^6 - 8.0 \times 10^6)t^{-0.58}$ (4.5 μm)
E (#/s)	Emission rate	–

[a]The breathing rate is obtained from the study of Kowalski.[59]

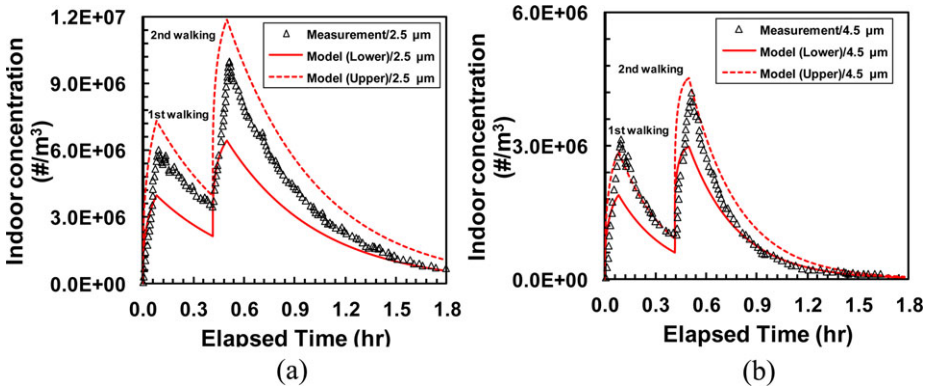

Fig. 2. The comparison between the model predictions and experimental data:[66] (a) 2–3 μm (denoted by 2.5 μm) and (b) 4–5 μm (denoted by 4.5 μm) particles.

larger resuspension rates than 4.5 μm particles. The predicting capability of the derived models for the case with WIPR is reasonably validated.

4. CASE STUDIES

The impact of resuspension on infection transmission was examined by two hypothetical case studies on bioterrorist attacks. In case 1 (AIPR case), pathogens were dosed onto the floor of a ventilation duct when the ventilation was off, and some of them were resuspended and transported into the indoor environment when the ventilation system was running again. In case 2 (WIPR case), pathogens were deposited onto an indoor floor and some of them were resuspended due to human walking. *B.*

anthracis was applied as the representative pathogen, which has the approximate size of 1 μm $\times$ 5 μm[67] in a rod shape corresponding to the aerodynamic diameter of 3 μm.[68] Although there are inhalational anthrax, cutaneous anthrax, and gastrointestinal anthrax in terms of exposure pathways, the inhalational anthrax is the most life-threatening one with a mortality rate as high as 90–99% if untreated.[69] This reinforces the importance of inhalation exposure analysis for *B. anthracis*.

4.1. Case 1—AIPR Case

Ten grams of *B. anthracis* spores were dosed onto the duct floor when the ventilation was off. It was assumed that a monolayer of spores was formed on the floor of the ventilation duct and the phenomena of clumping and aggregation that commonly occur for multiple deposits were neglected. Therefore, all deposited pathogen would be exposed to airflow when the ventilation was on and the results might represent an upper limit prediction for the considered bioterrorist attack case. The setting of parameters about the ventilation system, room geometry, and occupancy was similar to the study of You and Wan.[38] The initial indoor airborne and surface pathogen concentrations were zero. There were three occupants with a breathing rate of 2.83×10^{-4} m^3/s each.[59] The fraction of recirculated air, R_r, was 0.8.[33] The ventilation duct was made of plastic and had the cross-sectional dimension of 0.25 m (W) $\times$ 0.25 m (H).[33] The air exchange rate was 5 h^{-1}, corresponding to the flow rate of 800 m^3/h in the ventilation duct.[70] The friction velocity was estimated to be 0.247 m/s, according to the relationship between the friction velocity and free stream velocity in the study of You and Wan.[38] It was assumed that both dosed agents and recirculated agents would go through five bends before they entered indoors. The penetration coefficient of a bend (p_b) was approximately 100% for the considered airflow condition and size of agent.[52] The duct lengths from both the agent dosing location and the air outlet to the air supply intake were assumed to be 20 m. An ASHARE 40% filter of the efficiency of 0.8[51] for 3 μm particles (the average size for anthrax) was installed in the ventilation system. The parameters needed for calculating the normalized resuspension rate (Λ) and infection probability are listed in Tables II and III, respectively. The variation of airborne and surface pathogen concentrations and infection probability during a 4-h period for case 1 is shown by Fig. 3.

Table II. Parameters for Calculating the Normalized Resuspension Rate (Λ) of AIPR in Case 1

Parameters	Meaning	Unit	Value	Source
d_p	Particle diameter	μm	3	(67)
A_{132}	Hamaker constant	J	7.12×10^{-20}[a]	(25)
u^*	Friction velocity	m/s	0.247	(38)
ρ_p	Particle density	kg/m^3	1,200	(34)
ρ_a	Air density	kg/m^3	1.2	(68)
σ_1	Surface roughness	μm	5	(34)

[a] $A_{132} = \sqrt{A_{11} A_{22}}$, where $A_{11} = 6.5 \times 10^{-20}$ J and $A_{22} = 7.8 \times 10^{-20}$ J are the Hamaker constant of particle and surface, respectively.[25]

In case 1, the airborne pathogen concentration increases to the peak level of 4.95×10^5 #/m^3 at about 18 seconds and then declines quickly for up to about 7,200 seconds (2 hours) followed by a very slow decrease afterward. The airborne pathogen concentration only decreases by one-half (from 1800 #/m^3 to 900 #/m^3) for the period of 7,200–14,400 seconds (2–4 hours) compared to about two orders of magnitude for the period of 16–7,200 seconds (0.005–2 hours). This is because of the fact that the normalized resuspension rate of AIPR and time exhibits a power law decay correlation. The surface pathogen concentration increases all the way through 14,400 seconds (4 hours) because of the effect of deposition. The surface concentration increases very quickly before 1,800 seconds (0.5 hours) followed by a slow increase corresponding to the small airborne concentration then. The infection probability increases fast (from 0 to 0.54) during the first 1,800 seconds (0.5 hours) and increases relatively slowly (from 0.54 to 0.57) afterward. This suggests the importance of early evacuation action against a bioterrorist attack. The variation pattern of infection probability (Fig. 3(b)) is similar to that of surface concentration because human exposure to pathogens is directly related to the surface concentration in the case without WIPR as shown by Equation (16).

4.2. Case 2—WIPR Case

Ten grams of *B. anthracis* spores were deposited onto the floor of a mechanically ventilated room with carpet flooring. The corresponding initial surface pathogen concentration $M(0)$ was 4.61×10^9 #/m^2. The initial airborne pathogen concentration was zero. There were three occupants and it was assumed that there was averagely one occupant

Table III. Parameters Required for Estimating the Infection Probabilities of Two Case Studies

Parameter	Meaning	Case 1	Case 2
α_a (1/s)	Air exchange rate	1.39×10^{-3}	1.39×10^{-3}
p_c	Penetration through building shell	–	–
R_r	Fraction of recirculated air	0.8	0.8
η_r	Filter efficiency	0.8	0.8
p_b	Penetration through bend(s)	1	1
d_v	Deposition loss in the duct	0.98	0.98
v_{df} (m/s)	Deposition velocity onto floor	2.0×10^{-3}	2.0×10^{-3}
v_{dw} (m/s)	Deposition velocity onto wall	6.0×10^{-5}	6.0×10^{-5}
v_{dc} (m/s)	Deposition velocity onto ceiling	3.0×10^{-6}	3.0×10^{-6}
A_f (m^2)	Area of floor	64	64
A_w (m^2)	Area of wall	80	80
A_c (m^2)	Area of ceiling	64	64
V (m^3)	Volume of indoor space	160	160
β_b(m^3/s)	Breathing rate of occupants	2.83×10^{-4}	2.83×10^{-4}
n_p	Number of occupants	3	3
$C_i(0)$ (#/m^3)	Initial indoor airborne concentration	0	0
$M(0)$ (#/m^2)	Initial indoor surface concentration for resuspension	0	4.61×10^9
C_o (#/m^3)	Outdoor concentration	0	0
Λ (1/s)	Normalized resuspension rate for AIPR	$1.3 \times 10^{-3} t^{-0.97}$	–
R (#/s)	Resuspension rate WIPR	–	$3.60 \times 10^6 t^{-0.49}$
E (#/s)	Emission rate	–	–
p_{fi}	Inhalability parameter	1	1
γ_d (1/s)	Pathogen decay rate in air	2.27×10^{-8}[a]	2.27×10^{-8}[a]
r_i	Virulence coefficient of pathogen	7.15×10^{-6}[a]	7.15×10^{-6}[a]
ρ_p (kg/m^3)	Pathogen density	1,200[b]	1,200[b]

[a]The data are from Hong *et al.*[19]
[b]The data are from Krauter and Biermann.[34]

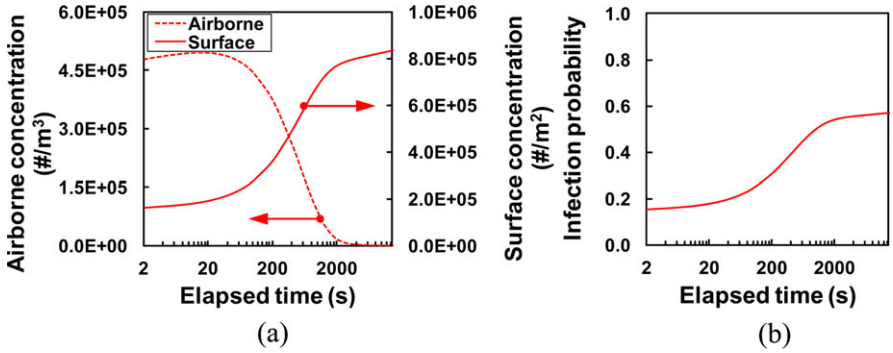

Fig. 3. Modeling results for case 1: the variation of (a) airborne and surface pathogen concentrations and (b) infection probability.

walking at the medium rate (e.g., 108 steps/min) during a 4-h period. The indoor RH was 40%. The resuspension area was assumed to be 20% of the total flooring area. Based on the carpet/PM_{10} case at the waking rate of 108 steps/min and the RH of 82% in the study of You and Wan,[45] the resuspension rate of the WIPR was approximated to be $R(t) = 61.07t^{-0.49}$ in the unit of μg/s. Considering the mass of a single spore for *B. anthracis*, $m_p = 1.696 \times 10^{-5}$ μg, the resuspension rate of the WIPR was $R(t) = (61.07/m_p)t^{-0.49} = 3.60 \times 10^6 t^{-0.49}$ in the unit of #/s. Values used for all other parameters are listed in Table III. Most of the parameters in this case had the same value as those used for case 1 except that: (1) the initial surface concentration is zero for case 1 whereas it is a finite value for case 2; (2) the normalized resuspension rate of AIPR is considered in case 1, whereas the resuspension rate of WIPR is considered in case 2. The modeling results are shown in Fig. 4.

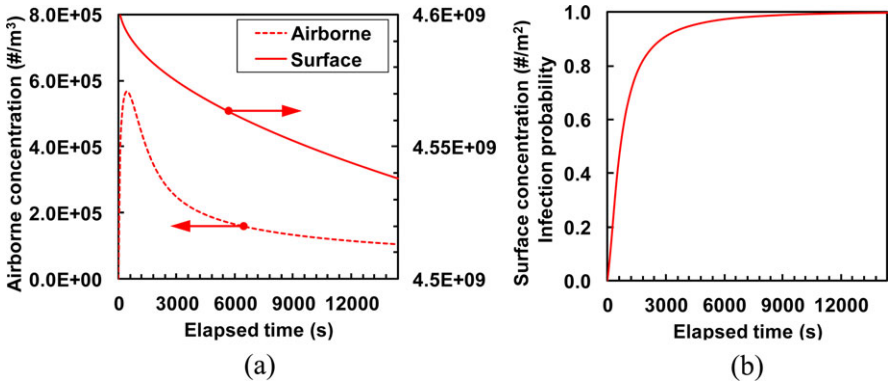

Fig. 4. Modeling results for case 2: the variation of (a) airborne and surface pathogen concentrations and (b) infection probability.

The WIPR increases the indoor airborne pathogen concentration to the peak level of 5.7×10^5 #/m^3 after about 400 seconds (0.11 hours) followed by the continuous decay that becomes slower and slower corresponding to the power law decrease of resuspension rate. The airborne pathogen concentrations at 7,200 seconds (2 hours), 10,800 seconds (3 hours), and 14,400 seconds (4 hours) are 1.50×10^5 #/m^3, 1.21×10^5 #/m^3, and 1.05×10^5 #/m^3, respectively. It could be expected that an approximate steady state for the indoor airborne concentration could be reached if the walking activity persists for longer time. The surface pathogen concentration decreases by 1.5% after 14,400 seconds (4 hours), showing the depletion effect of walking on the pathogens on the floor. The infection probability increases dramatically (from 0 to 0.87) during the first 1,800 seconds (0.5 hours) followed by a much slower increase afterward, suggesting that early identification of the bioterrorist attack and evacuation of occupants are critical for effectively mitigating an attack. After a 2-hour exposure, the infection probability is nearly 1, showing the capability of the WIPR to cause high infection risk.

Similar peak concentrations (4.95×10^5 #/m^3 vs. 5.7×10^5 #/m^3) are resultant for case 1 and case 2. However, the airborne concentration for case 2 reaches the peak later than case 1 (400 seconds vs. 18 seconds), and the airborne concentration in case 2 is significantly larger than that in case 1 (1.50×10^5 #/m^3 vs. 1,800 #/m^3) after 2 hours. This suggests the stronger capability of maintaining airborne pathogen concentration for the case with WIPR (case 2). Correspondingly, the infection probability of case 2 is higher than that of case 1 for a 4-hour exposure (1 vs. 0.57).

It should be noted that although two major resuspension scenarios (i.e., AIPR in the ventilation duct and WIPR indoors) are considered here, the proposed scheme could be easily extended to consider other resuspension processes (e.g., vacuum-cleaning-induced resuspension) by simply moderating the resuspension rate parameter in the concentration models (Equations (10) and (12)). Moreover, the proposed risk assessment scheme is also appropriate for the cases where no resuspension is involved, despite the impact of resuspension is specifically examined in this work. Hence, the risk assessment scheme could serve as an effective tool for the risk assessment of infection transmission indoors.

5. SENSITIVITY ANALYSIS

Sensitivity analysis was conducted by examining the effect of various factors on the infection probability based on the design-of-experiments (DOE) method with a 2^5 factorial design.[71] According to the airborne concentration model (Equation (10)), exposure model (Equation (15)), and dose-response model (Equation (17)), five factors including $A = a_2'$, $B = b$, $C = a_r/V$, $D = \beta_b p_{fi} p_{fs}$, and $E = r_i$ were considered. A combination of these factors covers all the parameters affecting infection probability. The factor A accounts for the effect of AIPR in the ventilation duct together with ventilation parameters (i.e., ventilation rate, filter efficiency, etc.). The factor B accounts for the effect of particle loss rate indoors. The factor C accounts for the effect of WIPR indoors. The fact or D accounts for the effect of the inspiratory rate of viable pathogens. The factor E accounts for the effect of the virulence coefficient of pathogen.

Table IV. 2^5 Factorial Design for Sensitivity Analysis

	Factors					
Run	$A = a_{r2}$	$B = b$	$C = a_r/V$	$D = \beta_b p_{fi} p_{fs}$	$E = r_i$	Response: P_i
1	−[a]	−	−	−	−	0.493
2	+	−	−	−	−	0.531
3	−	+	−	−	−	0.424
4	−	−	+	−	−	0.571
5	−	−	−	+	−	0.639
⋮	⋮	⋮	⋮	⋮	⋮	⋮
30	+	−	+	+	+	0.899
31	−	+	+	+	+	0.790
32	+	+	+	+	+	0.844

[a](+/−) signs represent the high and low levels of the factors, respectively.

In the factorial design, the effect of the factors on the infection probability P_i (600 seconds exposure) was examined and the low and high levels of the factors are ±20% of nominal values (i.e., A (18860.33#/(m^{3}s$^{1-r_{n2}}$)), B (0.002007 s^{-1}), C (22506.76 #/(m^{3}s$^{1-b_r}$)), D (0.000283 m^3/s), E (7.15×10^{-6})), respectively, in case 1 and case 2. The factorial layout is shown by Table IV, where (+/−) signs represent the high and low levels of the factors, respectively. The main effects and interactions of the factors are calculated by:

$$\text{Eff} = \frac{1}{2^4} \sum_{j=1}^{32} \pm P_{i,j}, \tag{18}$$

where ± corresponds to the (+/−) signs of each main effect and interaction for each response obtained from Table IV. The significance of the factors and their interactions on the response is analyzed by constructing a normal probability plot of the main effects and interactions as shown by Fig. 5. If a factor or an interaction has insignificant effect on the infection probability, it will behave like a small random error and will be normally distributed, as indicated by the straight line, whereas if a factor or an interaction has significant effect on the infection probability, it will deviate away from the line.[71] If a factor or an interaction is further away from the straight line, its effect will be more significant and the response will be more sensitive to it.

It is shown by Fig. 5 that the most significant effect is the main effects of D (14.12%) and E (14.12%), followed by the main effects of B (−7.17%), C (7.07%), and A (6.92%) (the negative sign means an inverse relationship). This means

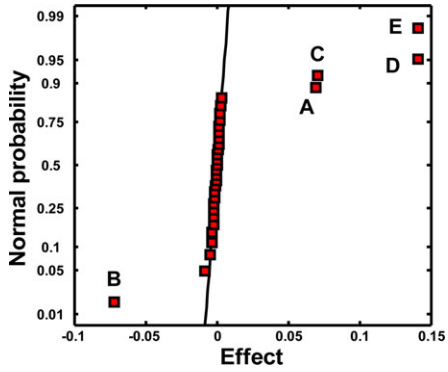

Fig. 5. Normal probability plot of the effects for the 2^5 factorial design.

that the infection probability is the most sensitive to the factors associated with the inspiration of viable pathogens (D) and pathogen virulence (E). The effect of the factors related to AIPR (A) in the duct and WIPR (C) indoors is comparable to the factor related to indoor particle loss mechanisms (B), all of which play a moderate role in the infection probability. This suggests that the infection control measures that are designed to reduce the inspiratory rate of viable pathogens (e.g., wearing mask and applying detergent to clean pathogen laden surfaces to reduce the number of viable pathogens on surfaces) and pathogen virulence (e.g., vaccines)[72] are the most effective, followed by the measures to increase the loss of airborne particle concentrations (e.g., increasing ventilation rate),[73] under the occurrence of AIPR or WIPR or both. The interactions of the factors have negligible effects compared to the main effects, as they well overlap with the straight line.

6. CONCLUSIONS

A new risk assessment scheme was developed to quantitatively explore the role of resuspension in indoor infection transmission. Two major resuspension scenarios (i.e., AIPR in ventilation ducts and WIPR indoors) were considered and a set of airborne and surface particle concentration models were derived based on the two-compartment mass balance models. Physical validation was conducted by comparing modeled airborne particle concentrations to the existing data found in the literature and a good agreement was found. The inhalation exposure analysis was conducted based on the derived airborne concentration model, which was subsequently incorporated into the dose-response model to assess the infection probability. Using the

proposed risk assessment scheme, the impact of resuspension to indoor infection transmission was examined by studying two hypothetical cases on bioterrorist attacks. Sensitivity analysis based on the DOE method showed that the factors that are related to the inspiratory rate of viable pathogens and pathogen virulence have the most significant effect on the infection probability, under the occurrence of AIPR and WIPR. The risk assessment scheme could serve as an effective tool for the risk assessment of an infection outbreak or a bioterrorist attack.

ACKNOWLEDGMENTS

Financial support was provided by the Republic of Singapore's National Research Foundation through a grant to the Berkeley Education Alliance for Research in Singapore (BEARS) for the Singapore-Berkeley Building Efficiency and Sustainability in the Tropics (SinBerBEST) Program. BEARS has been established by the University of California, Berkeley, as a center for intellectual excellence in research and education in Singapore.

REFERENCES

1. Corbett EL, Watt CJ, Walker N, Maher D, Williams BG, Raviglione MC, Dye C. The growing burden of tuberculosis: Global trends and interactions with the HIV epidemic. Archives of Internal Medicine, 2003; 163(9):1009–1021.
2. Kochi A. The global tuberculosis situation and the new control strategy of the World Health Organization. Bulletin of the World Health Organization, 2001; 79(1):71–75.
3. Pearson H, Clarke T, Abbott A, Knight J, Cyranoski D. SARS: What have we learned? Nature, 2003; 424(6945):121–126.
4. Radosavljević V, Jakovljević B. Bioterrorism—Types of epidemics, new epidemiological paradigm and levels of prevention. Public Health, 2007; 121(7):549–557.
5. Kaufmann AF, Meltzer MI, Schmid GP. The economic impact of a bioterrorist attack: Are prevention and postattack intervention programs justifiable? Emerging Infectious Diseases, 1997; 3(2):83–94.
6. Kousa A, Kukkonen J, Karppinen A, Aarnio P, Koskentalo T. A model for evaluating the population exposure to ambient air pollution in an urban area. Atmospheric Environment, 2002; 36(13):2109–2119.
7. Goldmann DA. Transmission of viral respiratory infections in the home. Pediatric Infectious Disease Journal, 2000; 19(10):S97–S102.
8. Li Y, Leung G, Tang J, Yang X, Chao C, Lin J, Lu J, Nielsen PV, Niu J, Qian H. Role of ventilation in airborne transmission of infectious agents in the built environment—A multidisciplinary systematic review. Indoor Air, 2007; 17(1):2–18.
9. Bean B, Moore B, Sterner B, Peterson L, Gerding D, Balfour H. Survival of influenza viruses on environmental surfaces. Journal of Infectious Diseases, 1982; 146(1):47–51.
10. Ferrier A, Garin D, Crance J. Rapid inactivation of vaccinia virus in suspension and dried on surfaces. Journal of Hospital Infection 2004; 57(1):73–79.
11. McDevitt JJ, Milton DK, Rudnick SN, First MW. Inactivation of poxviruses by upper-room UVC light in a simulated hospital room environment. PLoS One, 2008; 3(9):e3186.
12. Kent D, Reid D, Sokolowski J, Houk V. Tuberculin conversion: The iceberg of tuberculous pathogenesis. Archives of Environmental Health, 1967; 14(4):580–584.
13. Nazaroff WW. Norovirus, gastroenteritis, and indoor environmental quality. Indoor Air, 2011; 21(5):353–356.
14. Walter CW, Kundsin R. The floor as a reservoir of hospital infections. Surgery, Gynecology and Obstetrics, 1960; 111:412–422.
15. Goebes MD, Boehm AB, Hildemann LM. Contributions of foot traffic and outdoor concentrations to indoor airborne *Aspergillus*. Aerosol Science and Technology, 2011; 45(3):352–363.
16. Glover NJ. Countering chemical and biological terrorism. Civil Engineering, 2002; 72(5):62–67.
17. Armstrong T, Haas CN. A Quantitative microbial risk assessment model for legionnaires' disease: Animal model selection and dose-response modeling. Risk Analysis, 2007; 27(6):1581–1596.
18. Hong T, Gurian PL. Characterizing bioaerosol risk from environmental sampling. Environmental Science & Technology, 2012; 46(12):6714–6722.
19. Hong T, Gurian PL, Huang Y, Haas CN. Prioritizing risks and uncertainties from intentional release of selected Category A pathogens. PLoS One, 2012; 7(3):e32732.
20. Jones RM, Adida E. Influenza infection risk and predominate exposure route: Uncertainty analysis. Risk Analysis 2011; 31(10):1622–1631.
21. Jones RM, Masago Y, Bartrand T, Haas CN, Nicas M, Rose JB. Characterizing the risk of infection from Mycobacterium tuberculosis in commercial passenger aircraft using quantitative microbial risk assessment. Risk Analysis, 2009; 29(3):355–365.
22. Nicas M, Jones RM. Relative contributions of four exposure pathways to influenza infection risk. Risk Analysis, 2009; 29(9):1292–1303.
23. Nicas M, Sun G. An integrated model of infection risk in a healthcare environment. Risk Analysis, 2006; 26(4):1085–1096.
24. Price PN, Sohn MD, LaCommare KS, McWilliams JA. Framework for evaluating anthrax risk in buildings. Environmental Science & Technology, 2009; 43(6):1783–1787.
25. Kim Y, Gidwani A, Wyslouzil BE, Sohn CW. Source term models for fine particle resuspension from indoor surfaces. Building and Environment, 2010; 45(8):1854–1865.
26. Loosmore GA. Evaluation and development of models for resuspension of aerosols at short times after deposition. Atmospheric Environment, 2003; 37(5):639–647.
27. Reeks M, Reed J, Hall D. On the resuspension of small particles by a turbulent flow. Journal of Physics D: Applied Physics, 1988; 21:574–589.
28. Bagnold RA. The Physics of Blown Sand and Desert Dunes. London: Methuen Publishing, 1941.
29. Braaten DA. Wind tunnel experiments of large particle reentrainment-deposition and development of large particle scaling parameters. Aerosol Science and Technology, 1994; 21(2):157–169.
30. Roney JA, White BR. Estimating fugitive dust emission rates using an environmental boundary layer wind tunnel. Atmospheric Environment, 2006; 40(40):7668–7685.
31. Ziskind G, Fichman M, Gutfinger C. Resuspension of particulates from surfaces to turbulent flows—Review and analysis. Journal of Aerosol Science, 1995; 26(4):613–644.
32. Lai ACK, Nazaroff WW. Modeling indoor particle deposition from turbulent flow onto smooth surfaces. Journal of Aerosol Science, 2000; 31(4):463–476.
33. Sippola MR, Nazaroff WW. Modeling particle loss in ventilation ducts. Atmospheric Environment, 2003; 37(39):5597–5609.

34. Krauter P, Biermann A. Reaerosolization of fluidized spores in ventilation systems. Applied and Environmental Microbiology, 2007; 73(7):2165–2172.
35. Sansone EB, Slein MW. Redispersion of indoor surface contamination: A review. Journal of Hazardous Materials, 1977; 2(4):347–361.
36. Zuraimi M. Is ventilation duct cleaning useful? A review of the scientific evidence. Indoor Air. 2010; 20(6):445–457.
37. Thompson BP, Bank LC. Survey of bioterrorism risk in buildings. Journal of Architectural Engineering, 2008; 14(1):7–17.
38. You S, Wan MP. Particle concentration dynamics in the ventilation duct after an artificial release: For countering potential bioterrorist attack. Journal of Hazardous Materials, 2014; 267:183–193.
39. Lehtonen M, Reponen T, Nevalainen A. Everyday activities and variation of fungal spore concentrations in indoor air. International Biodeterioration & Biodegradation, 1993; 31(1):25–39.
40. Crawford C, Reponen T, Lee T, Iossifova Y, Levin L, Adhikari A, Grinshpun SA. Temporal and spatial variation of indoor and outdoor airborne fungal spores, pollen, and (1,3)-D-glucan. Aerobiologia 2009; 25(3):147–158.
41. Buttner MP, Stetzenbach LD. Monitoring airborne fungal spores in an experimental indoor environment to evaluate sampling methods and the effects of human activity on air sampling. Applied and Environmental Microbiology, 1993; 59(1):219–226.
42. Jo WK, Seo YJ. Indoor and outdoor bioaerosol levels at recreation facilities, elementary schools, and homes. Chemosphere, 2005; 61(11):1570–1579.
43. Qian J, Peccia J, Ferro AR. Walking-induced particle resuspension in indoor environments. Atmospheric Environment, 2014; 89:464–481.
44. Weis CP, Intrepido AJ, Miller AK, Cowin PG, Durno MA, Gebhardt JS, Bull R. Secondary aerosolization of viable *Bacillus anthracis* spores in a contaminated US Senate Office. JAMA, 2002; 288(22):2853–2858.
45. You S, Wan MP. Experimental investigation and modelling of human-walking-induced particle resuspension. Indoor and Built Environment, 2014:1420326X14526424.
46. Ferro AR, Kopperud RJ, Hildemann LM. Source strengths for indoor human activities that resuspend particulate matter. Environmental Science & Technology, 2004; 38(6):1759–1764.
47. Chen Q, Hildemann LM. The effects of human activities on exposure to particulate matter and bioaerosols in residential homes. Environmental Science & Technology, 2009; 43(13):4641–4646.
48. Hussein T, Korhonen H, Herrmann E, Hämeri K, Lehtinen KE, Kulmala M. Emission rates due to indoor activities: Indoor aerosol model development, evaluation, and applications. Aerosol Science and Technology, 2005; 39(11):1111–1127.
49. Nazaroff WW, Cass GR. Mathematical modeling of indoor aerosol dynamics. Environmental Science & Technology, 1989; 23(2):157–166.
50. Schneider T, Kildes J. A two compartment model for determining the contribution of sources, surface deposition and resuspension to air and surface dust concentration levels in occupied rooms. Building and Environment, 1999; 34(5):583–595.
51. Riley WJ, McKone TE, Lai AC, Nazaroff WW. Indoor particulate matter of outdoor origin: Importance of size-dependent removal mechanisms. Environmental Science & Technology, 2002; 36(2):200–207.
52. McFarland A, Gong H, Muyshondt A, Wente W, Anand N. Aerosol deposition in bends with turbulent flow. Environmental Science & Technology, 1997; 31(12):3371–3377.
53. Lai ACK. Particle deposition indoors: A review. Indoor Air 2002; 12(4):211–214.
54. Heyder J, Gebhart J, Rudolf G, Schiller CF, Stahlhofen W. Deposition of particles in the human respiratory tract in the size range 0.005–15 μm. Journal of Aerosol Science, 1986; 17(5):811–825.
55. Long CM, Suh HH, Catalano PJ, Koutrakis P. Using time-and size-resolved particulate data to quantify indoor penetration and deposition behavior. Environmental Science & Technology, 2001; 35(10):2089–2099.
56. Chan AT. Indoor–outdoor relationships of particulate matter and nitrogen oxides under different outdoor meteorological conditions. Atmospheric Environment, 2002; 36(9):1543–1551.
57. Hussein T, Glytsos T, Ondráček J, Dohányosová P, Ždímal V, Hämeri K, Lazaridis M, Smolík J, Kulmala M. Particle size characterization and emission rates during indoor activities in a house. Atmospheric Environment, 2006; 40(23):4285–4307.
58. Afshari A, Matson U, Ekberg LE. Characterization of indoor sources of fine and ultrafine particles: A study conducted in a full-scale chamber. Indoor Air, 2005; 15(2):141–150.
59. Kowalski WJ. Immune Building Systems Technology. McGraw Hill Professional, 2003.
60. Nazaroff WW, Nicas M, Miller SL. Framework for evaluating measures to control nosocomial tuberculosis transmission. Indoor Air, 1998; 8(4):205–218.
61. Sze To G, Chao C. Review and comparison between the Wells–Riley and dose-response approaches to risk assessment of infectious respiratory diseases. Indoor Air, 2010; 20(1):2–16.
62. Beggs C, Noakes C, Sleigh P, Fletcher L, Siddiqi K. The transmission of tuberculosis in confined spaces: An analytical review of alternative epidemiological models. International Journal of Tuberculosis and Lung Disease, 2003; 7(11):1015–1026.
63. Weber TP, Stilianakis NI. Inactivation of influenza A viruses in the environment and modes of transmission: A critical review. Journal of Infection, 2008; 57(5):361–373.
64. Millage KK, Bergman J, Asgharian B, McClellan G. A review of inhalability fraction models: Discussion and recommendations. Inhalation Toxicology, 2010; 22(2):151–159.
65. Haas CN, Rose JB, Gerba CP. Quantitative Microbial Risk Assessment. New York: John Wiley & Sons, 1999.
66. Qian J, Ferro AR. Resuspension of dust particles in a chamber and associated environmental factors. Aerosol Science and Technology, 2008; 42(7):566–578.
67. Inglesby TV, Henderson DA, Bartlett JG, Ascher MS, Eitzen E, Friedlander AM, Hauer J, McDade J, Osterholm MT, O'Toole T. Anthrax as a biological weapon. JAMA, 1999; 281(18):1735–1745.
68. Hinds WC. Aerosol Technology: Properties, Behavior, and Measurement of Airborne Particles, 2nd ed. Hoboken, NJ: John Wiley & Sons, 2012.
69. Jernigan JA, Stephens DS, Ashford DA, Omenaca C, Topiel MS, Galbraith M, Tapper M, Fisk TL, Zaki S, Popovic T. Bioterrorism-related inhalational anthrax: The first 10 cases reported in the United States. Emerging Infectious Diseases, 2001; 7(6):933–944.
70. Wu PC, Li YY, Chiang CM, Huang CY, Lee CC, Li FC, Su HJ. Changing microbial concentrations are associated with ventilation performance in Taiwan's air-conditioned office buildings. Indoor Air, 2005; 15(1):19–26.
71. Montgomery DC. Design and Analysis of Experiments. Hoboken, NJ: John Wiley & Sons, 2008.
72. Gandon S, Mackinnon MJ, Nee S, Read AF. Imperfect vaccines and the evolution of pathogen virulence. Nature, 2001; 414(6865):751–756.
73. Gilkeson C, Camargo-Valero M, Pickin L, Noakes C. Measurement of ventilation and airborne infection risk in large naturally ventilated hospital wards. Building and Environment, 2013; 65:35–48.